

光电工程

Opto-Electronic Engineering

中文核心期刊 中国科技核心期刊
Scopus CSCD

飞秒激光制备柔性电子器件进展

廖嘉宁, 张东石, 李铸国

引用本文:

廖嘉宁, 张东石, 李铸国. 飞秒激光制备柔性电子器件进展[J]. 光电工程, 2022, 49(2): 210388.

Liao J N, Zhang D S, Li Z G. Advance in femtosecond laser fabrication of flexible electronics[J]. *Opto-Electron Eng*, 2022, 49(2): 210388.

<https://doi.org/10.12086/oee.2022.210388>

收稿日期: 2021-11-30; 修改日期: 2022-02-11

相关论文

飞秒激光加工微纳光学器件

董彬, 张娟, 王达伟, 张亦元, 张乐然, 李瑞, 辛晨, 刘顺利, 张子航, 吴昊, 蒋绍军, 朱苏皖, 刘炳瑞, 吴东
光电工程 2023, 50(3): 220073 doi: [10.12086/oee.2023.220073](https://doi.org/10.12086/oee.2023.220073)

飞秒激光时空整形的电子动态调控微孔加工

张超, 李敏, 叶柏臣, 吴剑英, 王智, 李晓炜
光电工程 2022, 49(2): 210389 doi: [10.12086/oee.2022.210389](https://doi.org/10.12086/oee.2022.210389)

飞秒激光直写加工SERS基底及其应用

尹智东, 倪才鼎, 吴思竹, 劳召欣
光电工程 2023, 50(3): 220322 doi: [10.12086/oee.2023.220322](https://doi.org/10.12086/oee.2023.220322)

飞秒激光双光子聚合三维微纳结构加工技术

赵圆圆, 金峰, 董贤子, 郑美玲, 段宣明
光电工程 2023, 50(3): 220048 doi: [10.12086/oee.2023.220048](https://doi.org/10.12086/oee.2023.220048)

更多相关论文见光电期刊集群网站 



<http://cn.oejournal.org/oee>



OE_Journal



Website

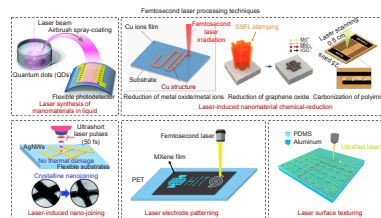


DOI: 10.12086/oee.2022.210388

飞秒激光制备柔性电子器件进展

廖嘉宁, 张东石*, 李铸国*

上海交通大学材料科学与工程学院, 上海市激光制造与材料改性重点实验室, 焊接与激光制造研究所, 上海 200240



摘要: 消费电子市场正推动柔性电子器件向集成化、小型化及可穿戴的方向发展,同时也对柔性电子器件的制备提出了新的要求。光刻工艺加工精度高,但其成本昂贵、加工流程复杂且效率低。相比而言,飞秒激光加工兼有加工精度高和工艺流程简单的特点,已展现在制备柔性电子器件方面的独特优势和应用前景。为了更好地了解这一新兴领域的进展,本文概述了与柔性电子器件制备相关的五种飞秒激光加工工艺机理,包括激光液相纳米材料合成、激光纳米材料还原、激光诱导纳米连接、激光电极图案化及激光表面织构化,并介绍了制备的典型柔性电子器件性能,对存在的问题和未来发展趋势进行了分析和展望。

关键词: 飞秒激光; 微纳加工; 柔性电子; 纳米材料连接; 纳米材料制备

中图分类号: TN249

文献标志码: A

廖嘉宁, 张东石, 李铸国. 飞秒激光制备柔性电子器件进展 [J]. 光电工程, 2022, 49(2): 210388
Liao J N, Zhang D S, Li Z G. Advance in femtosecond laser fabrication of flexible electronics[J]. *Opto-Electron Eng*, 2022, 49(2): 210388

Advance in femtosecond laser fabrication of flexible electronics

Liao Jianing, Zhang Dongshi*, Li Zhuguo*

Shanghai Key Laboratory of Materials Laser Processing and Modification, School of Materials Science and Engineering, Shanghai Jiao Tong University, Shanghai 200240, China

Abstract: Consumer electronical markets are now promoting a rapid advance in flexible electronics with high integration, miniaturization, and wearable properties, which in turn puts forward new requirements for the fabrication of flexible electronics. Photolithography techniques are advantageous for their high accuracy, but it is disadvantageous due to high cost, complexity, and low efficiency. In comparison, femtosecond (fs) laser micro-nano fabrication, as a high-efficiency and simple technique, has shown its capacity and potential for the fabrication of flexible electronics. This review summarizes five fs-laser based techniques for the fabrication of flexible electronics, including laser synthesis of nanomaterials in liquids, laser-induced nanomaterial chemical-reduction, laser-induced nano joining, laser electrode patterning, and laser surface texturing. The corresponding mechanisms are briefly introduced, followed by a demonstration of typical flexible electronics and their properties. Finally, the challenges in this field are analyzed, and our perspective is provided.

Keywords: femtosecond laser; micro-nano fabrication; flexible electronics; nanojoining; nanomaterial synthesis

收稿日期: 2021-11-30; 收到修改稿日期: 2022-02-11

基金项目: 上海交通大学长聘教轨副教授科研启动费 (WF220405017)

*通信作者: 张东石, zhangdongshi@sjtu.edu.cn; 李铸国, lizg@sjtu.edu.cn。

版权所有©2022 中国科学院光电技术研究所

1 引言

随着信息技术的快速发展和消费电子的兴起, 高便携、轻量化的柔性电子器件受到了越来越多的关注^[1-2]。柔性电子器件由功能结构、导电结构及柔性基板三部分构成。功能结构可响应外界刺激如温度、湿度、应力、应变及化学介质等并将其转化为电信号; 导电结构用于电信号的传输; 柔性基板则用于支撑功能结构与导电结构。

纳米材料具有高的比表面积、多的活性位点及量子尺寸效应, 展现出优异的机械、光学、电学及催化性能, 在高性能电子器件制造中具有极大应用前景^[3]。金属纳米材料多用于导电结构, 而碳材料/半导体纳米材料多用于功能结构。纳米材料的合成方法可被分为“自上而下”及“自下而上”两大类^[4]。“自上而下”法是指将块状材料转化为纳米材料, 包括机械球磨法、溅射法等。“自下而上”法则从较小结构单元(原子、分子尺度)出发, 自组装形成纳米材料, 包括湿化学法、化学气相沉积法、激光还原法等^[4]。将合成的纳米材料收集、转移、加工并图案化才能制造柔性电子器件。常用的图案化技术有光刻^[5]和喷墨打印^[6]。光刻工艺在制备最小特征尺寸和高分辨率柔性器件方面优势巨大, 但其耗时长、需掩膜板, 加工过程中易引入有毒化学物质破坏纳米结构, 工艺流程复杂, 灵活性差、不适用于小批量制造^[7]。喷墨打印是非接触式方法, 无需掩膜, 灵活可控性高, 但其加工精度低、可印刷油墨制备复杂, 并需烧结后处理工艺来制备导电结构, 易破坏热敏基板^[8]。

连续激光^[9-10]和脉冲激光^[11]微纳加工, 不仅可以实现从块体靶材到原子/分子尺度材料的制备^[12], 还可以实现从原子/分子尺度到纳米材料^[13-15]和微纳结构^[16-19]的材料自组装。激光加工是无掩膜版工艺, 在工艺灵活性方面, 可进行材料合成^[20-23]和烧结^[24]、表面改性^[25-26]、表面织构化^[27-31]及图案化^[32-33], 甚至可以一步快速制备完整的柔性器件^[34], 还可实现同一类型或不同类型功能单元在同一基板上的快速集成^[35-36]。连续激光热效应显著, 可诱导石墨烯化^[37]及实现金属纳米材料大面积烧结^[9], 但加工结构图案分辨率低、易损伤柔性基板^[38]。脉冲激光, 特别是飞秒激光, 由于脉宽短、峰值功率高及热效应小^[12], 不仅可实现无损或低损微纳结构的高分辨图案“冷”加工, 还可实现多维度纳米材料的合成和连接, 可用于柔性电子器

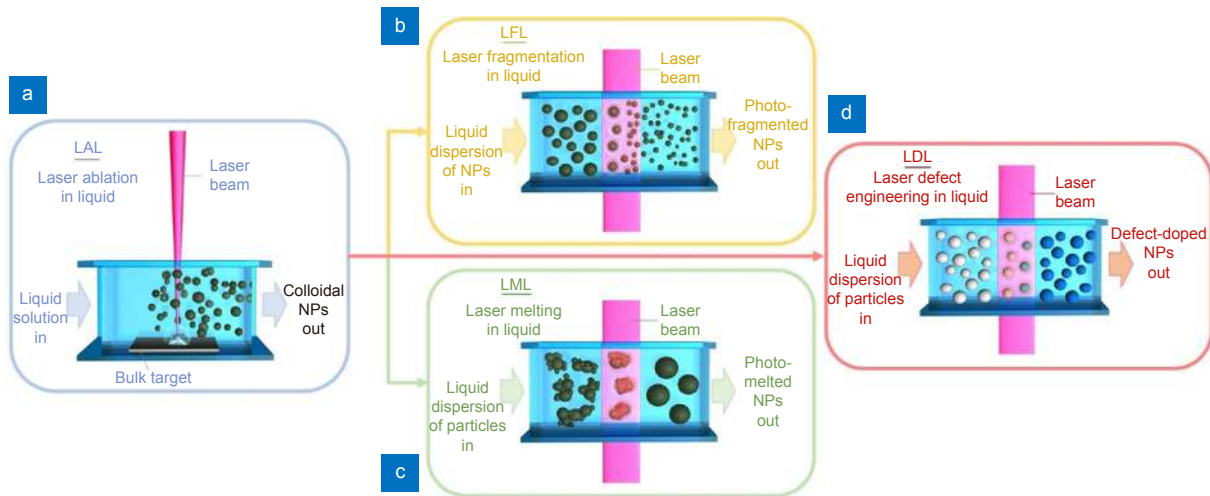
件制造^[28,39-40]。本文将从加工工艺和器件性能两个方面介绍五种飞秒激光制备柔性电子器件电极材料的工艺方法及其相关机理, 包括飞秒激光液相纳米材料合成、飞秒激光纳米材料还原、飞秒激光纳米材料连接、飞秒激光电极图案化和飞秒激光表面织构化, 并对比基于相关工艺构建的典型柔性电子器件的性能, 最后总结该领域现存技术挑战和未来发展趋势。

2 飞秒激光加工工艺及应用

2.1 飞秒激光液相纳米材料合成

激光合成纳米材料可在真空、气体、液体三种环境下进行。液体是合成纳米材料最有利的环境, 可在室温大气压下进行, 过程绿色无污染, 具有极端的局部热力学条件, 可诱导产生高温高压环境和材料的急速冷却, 导致材料的氧化、碳化、硫化、氮化和复合化, 实现纳米材料多样性合成^[41-42]。相较于传统湿化学法, 由于没有配体的限制, 利用激光液相合成纳米颗粒具有更高的清洁度, 可实现表面100%密度的生物材料接枝并展现了比化学合成材料更高的催化活性^[42]。由于激光合成的胶体分散性好, 无需后处理(如离心、清洗)过程, 易转移到其他基板, 可替代化学方法合成的材料用于柔性器件构造。虽然其在柔性电子器件的交叉学科研究报道不多, 但是参考化学合成材料在柔性电子应用的现状, 其前景还是比较光明的。

根据合成场景和目的不同, 可将激光液相合成细分为激光液相烧蚀(LAL, 图1(a))、激光液相碎裂(LFL, 图1(b))、激光液相熔合(LML, 图1(c))、激光液相缺陷工程(LDL, 图1(d))^[20]。激光液相烧蚀(LAL)是利用激光将固体靶材在液相环境下转化为纳米材料, 在没有抑制剂抑制晶体成核和生长的情况下, 获得的纳米胶体粒径范围大^[43-44], 虽可以直接使用, 但不能用于研究纳米材料的尺寸效应。激光液相碎裂工艺(LFL)是将液体中分散的纳米尺度或微米尺度的颗粒通过高能激光碎裂成更小尺度的纳米材料, 使其具有更大的比表面积和活性, 适用于能源^[45-46]、光电检测^[47]、催化^[48]、生物杀菌^[49]等领域。激光液相熔合(LML)可以将团簇胶体颗粒通过激光的光热效应融合成大尺寸颗粒^[50], 通常采用纳秒激光, 而超快激光尤其是飞秒激光由于其“冷效应”, 鲜有报道。激光液相缺陷工程(LDL)则是通过激光辐照诱导产生大量缺陷以改变颗粒的原子结构, 可用于高性能纳米催化剂

图 1 激光液相合成及处理工艺示意图^[20]。

(a) 激光液相烧蚀 (LAL); (b) 激光液相碎裂 (LFL); (c) 激光液相熔合 (LML); (d) 激光液相缺陷工程 (LDL)

Fig. 1 Schematic diagram of the laser synthesis and treatment in liquid^[20].

- (a) Laser ablation in liquid (LAL); (b) Laser fragmentation in liquid (LFL);
- (c) Laser melting in liquid (LML); (d) Laser defect-engineering in liquid (LDL)

的制备^[51]。LFL、LML 及 LDL 可作为 LAL 合成材料的后处理工艺调控其尺寸、成分和缺陷。LAL 作为 LFL、LML 及 LDL 工艺的初始环节，也是块体材料向纳米材料转化的关键步骤。

飞秒激光液相烧蚀制备纳米材料涉及复杂的物理化学过程，目前其反应的详细机理仍不明晰，下面对其做简单介绍。首先，飞秒激光在经过液体时会发生反射、折射、自聚焦和光学击穿现象，从而影响焦点位置和激光到达靶材的能量密度，进而对其烧蚀过程产生影响^[52-53]。当飞秒激光辐照到固体靶材时，材料载流子吸收脉冲能量并达到较高温度，如金属中自由电子、半导体或绝缘体的价带电子。根据双温模型，这些被电子吸收的能量在几皮秒后通过电子-电子和电子-声子碰撞传输到晶格，使靶材局部温度急剧升高，最终达到新的平衡态^[54-55]。激光与物质作用机制主要包括库伦爆炸、相爆炸及等离子体烧蚀^[54,56]，依次发生在低功率密度、高功率密度和更高功率密度^[57]。库伦爆炸机制为：靶材吸收激光脉冲的能量使电子通过光电及热电发射从靶材表面逸出，并在表面形成高强度电场，该电场将导致正离子间强烈静电排斥，从而发生库伦爆炸使材料碎裂并形成纳米颗粒^[58]。相爆炸机制为：飞秒激光与靶材作用时，靶材表面被迅速加热到临界温度以上，使靶材表面过热形成过热液层并极速分解成蒸汽、原子团簇和液滴混合物，迅速膨胀喷射离开靶材，对于飞秒激光来说，这是一个等容

加热和快速绝热膨胀的过程^[59]。水与过热金属接触的部分会进入超临界状态，并导致低密度金属-液体混合区的形成，该混合区是随后产生的空化气泡的前驱体。混合区有利于蒸发产生的金属原子凝结为最大不超过十纳米的颗粒，同时过热液态金属层的分解会产生数十纳米尺度的颗粒^[60]。Lasemi 等^[61]在飞秒激光烧蚀正己烷中镀金镍靶后，观察到了可能由于相爆炸发生导致金属液滴溅射凝固后的表面结构。等离子体烧蚀机制为：当激光功率密度超过等离子形成阈值时，材料直接电离和升华，电子发射形成高温高压的等离子体羽流，实现固体靶材到等离子体的直接转化^[62]，还可实现溶液分子的分解。等离子体羽流是由高度离子化的靶材电子、原子、离子组成，在高温高压环境下可诱导原子之间的相互反应，生成氧化物、碳化物、氢氧化物等多种纳米材料的前驱体。随着等离子体羽流的膨胀可导致激光诱导冲击波的产生，在冲击波前端，大的压力梯度以及等离子体和周围液体强烈热交换可以导致气泡产生^[63]。气泡中包含溶液分解产生的气体及靶材汽化产生的各种原子、团簇和反应生成物的前驱体^[64]。随着气泡的膨胀和收缩，这些物质会发生碰撞，纳米颗粒尺寸有所变化。气泡破裂后所合成的纳米颗粒便会分散在溶液中^[54,65]，由于颗粒具有高活性，在液体环境下还会继续生长^[43-44,66]。

与纳秒、微秒激光相比，飞秒激光液相烧蚀具有独特优势。1) 飞秒激光在焦点处峰值功率远高于纳秒

/微秒激光, 可构建更高温度和更高压强的极端局部环境, 有利于亚稳相的形成^[67-69]。2) 飞秒激光热效应不明显, 可制备尺寸更小的纳米材料。Camarda 等^[70]发现了纳秒激光合成的 ZnO NPs 平均粒径约为 30 nm, 而飞秒激光合成的 ZnO NPs 平均粒径则小于 10 nm。ZnO 为宽带隙 (3.3 eV) 半导体材料, 具有高激子结合能 (60 meV), 在紫外光电探测器中有广泛应用^[71]。Mirtra 等人^[72]在乙醇溶液中利用飞秒激光烧蚀氮化锌靶 (Zn_3N_2) 制备了稳定的碳掺杂氧化锌量子点 (ZnO QDs) 胶体溶液, 并将其喷涂在叉指钛电极表面, 经过烘干处理制备了高性能的柔性深紫外光电探测器 (图 2(a)), 对深紫外光具有高的瞬态光电流响应 88.4 mA/W (图 2(b)), 在 30° 下循环弯折 150 次后, 所制备的光电器件的响应率基本未改变 (图 2(c)), 显示良好的柔性和光电稳定性。

2.2 飞秒激光纳米材料还原

2.2.1 还原制备金属纳米材料

金属纳米材料, 如金 (Au)、银 (Ag)、铜 (Cu) 等通常用作柔性器件电极材料或传感材料。飞秒激光在较低脉冲能量下即可将金属氧化物纳米材料或离子态金属盐前驱体还原为金属纳米颗粒^[21-22,39]。相比于贵金属, Cu 成本更低, 由其制成的柔性电子器件具有更高的经济效益^[9]。飞秒激光可在还原剂辅助下将氧化铜纳米颗粒 (CuO NPs) 还原为 Cu NPs, 并将其烧结成导电铜电极。常用的还原剂包括含羟基的醇类 (如乙二醇^[73])、分解后可产生羧酸的有机物 (如聚乙烯吡咯烷酮^[74])。以乙二醇为例, 飞秒激光辐照后, CuO NPs 前驱体温度会不断升高, 当温度达到乙二醇沸点 197.3 °C 时, 乙二醇脱水生成乙醛, 乙醛将 CuO NPs 还原为 Cu NPs, 反应式如下^[73]:

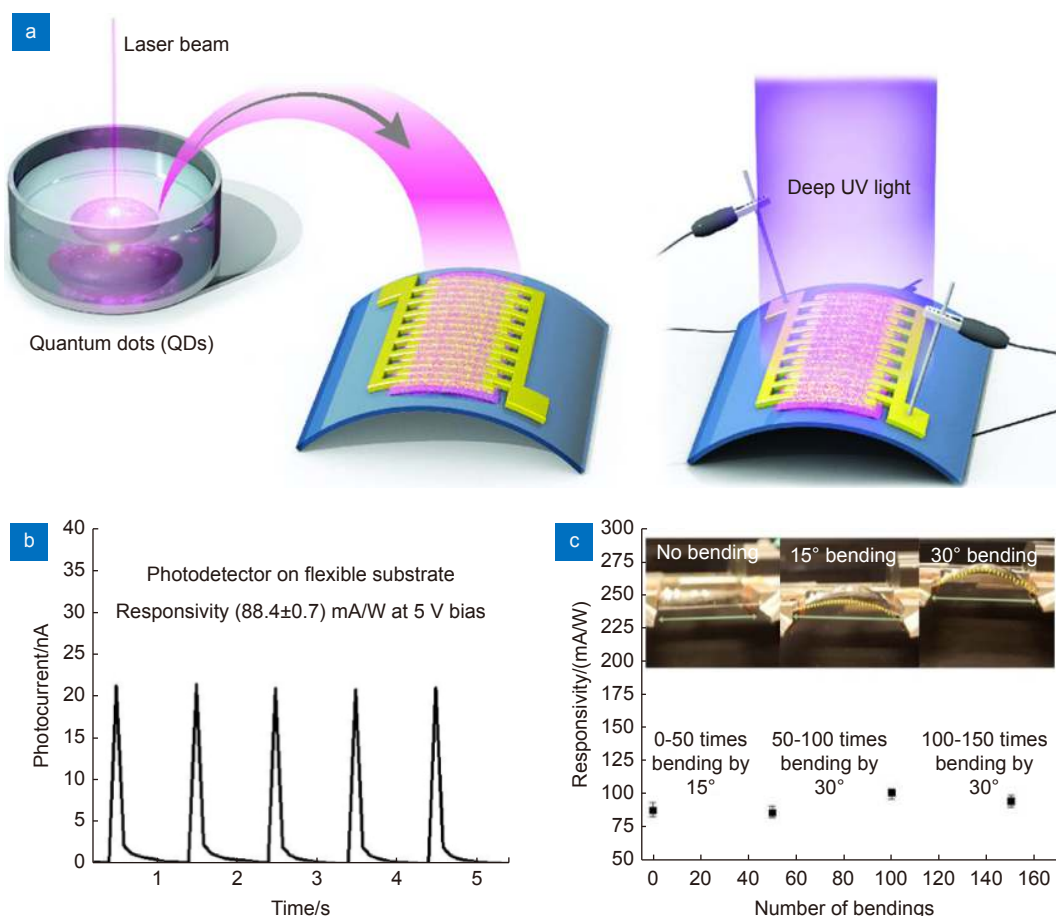
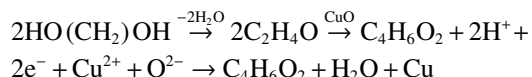


图 2 (a) 飞秒激光烧蚀合成氧化锌量子点制备光电探测器示意图; (b) 深紫外光下光电探测器的瞬时光电流产生;
(c) 光电探测器的响应值随器件弯曲角度、次数变化关系, 插图为光电探测器弯曲角度的照片^[72]

Fig. 2 (a) Schematic illustration of femtosecond laser ablation synthesis with ZnO QDs to fabricate photodetectors; (b) Transient photocurrent generation under deep-ultraviolet illumination for photodetector; (c) Responsivity measurement of photodetector as a function of the number of bending cycles. The inset photos show the photodetector bending degree^[72]



调控飞秒激光参数可控制 CuO NPs 的还原程度, 制备不同 Cu/Cu₂O 比例的复合微型温度传感器^[75-76]。飞秒激光还原离子态铜盐前驱体制备铜微电极流程, 如图 3(a) 所示。当飞秒激光辐照离子态铜盐前驱体时, 前驱体中还原剂(聚乙烯吡咯烷酮 PVP)发生光分解生成无定形碳、亚甲基、甲胺和丙酸^[74]。丙酸可进一步被分解形成甲酸, 从而将铜离子还原为铜纳米颗粒^[77]。可调控激光功率及扫描速度对铜微电极的微观结构及化学成分(图 3(b), 3(c))实现对电极电阻的调控^[39,77]。以激光功率为例, 较小激光功率(≤ 322 mW), 少量 Cu²⁺被还原为 Cu 纳米颗粒, 不能形成导电网络, 所以电阻高; 在激光功率为 626 mW~960 mW 时,

更多 Cu²⁺被还原为 Cu⁺及 Cu 纳米材料, 并连接成导电性良好的导电网络; 继续增加激光功率会导致还原的 Cu 颗粒被氧化为氧化亚铜(Cu₂O)且使颗粒尺寸增大弱化连接效果, 所以电极方阻升高(图 3(d))^[39]。最优的激光功率为 960 mW, 此时的电阻约为 11.2 $\Omega \cdot \text{sq}^{-1}$, 该条件下制备的 Cu 电极柔性良好, 在弯折半径为 2.3 cm 时, 电阻变化率仅为 2.9%, 可制成 LED 电路(图 3(d) 插图)^[39]。

在还原剂的作用下, 利用飞秒激光还可实现离子态金、银和多金属离子比如 Ag⁺/Pd²⁺的还原, 得到 Au、Ag 纳米颗粒^[78-79]和 Ag/Pd 合金纳米材料^[80]。不同组分比例的 Ag/Pd 合金纳米结构可制成柔性 SERS 传感器^[80], 当 Pd 含量为 18% 时, 所制备 SERS 传感器的增强因子可达 2.62×10^8 , 对 R6G 污染物的检测

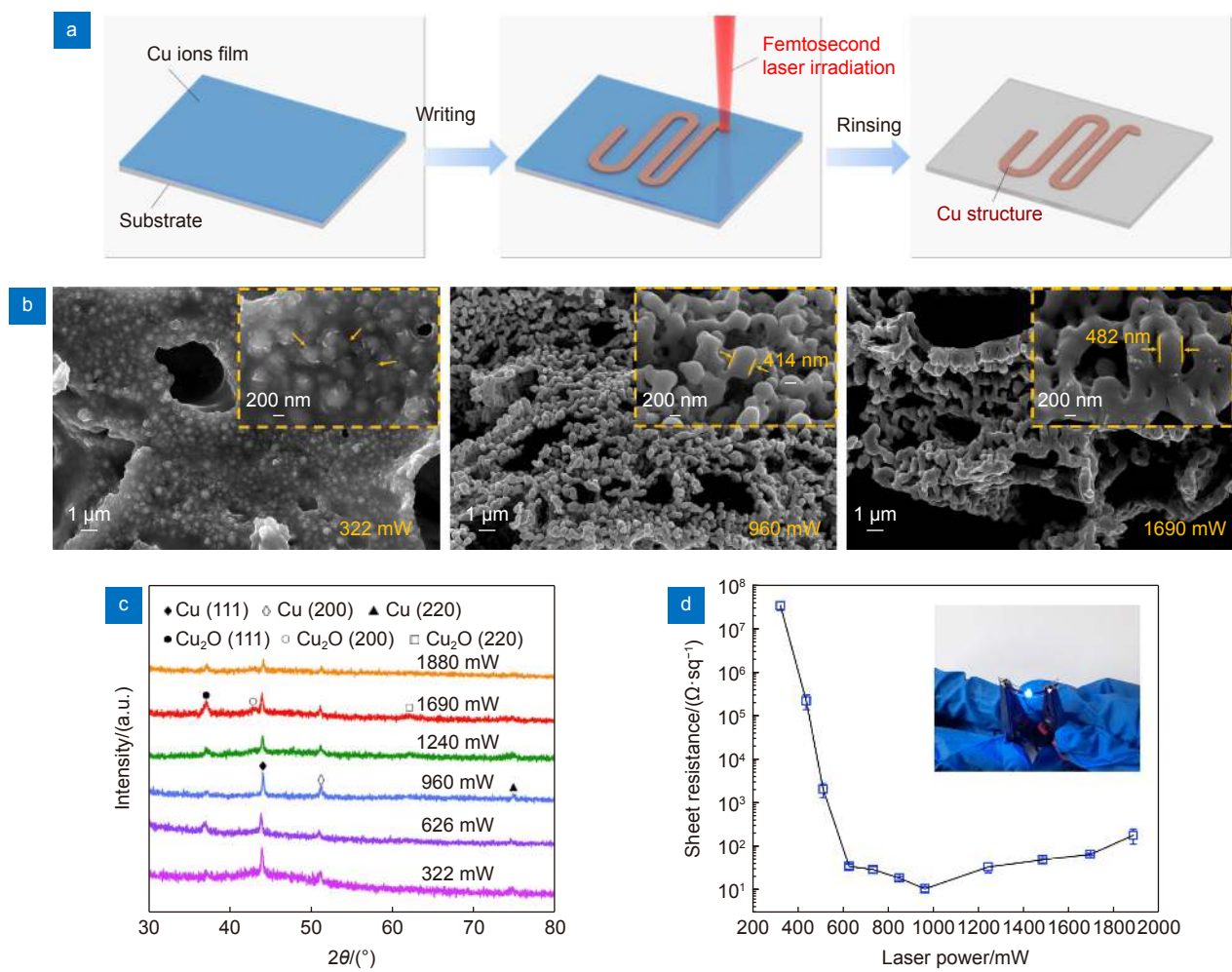


图 3 (a) 飞秒激光还原离子态铜盐前驱体制备铜微电极流程图; (b), (c) 不同激光功率下制备铜微电极的 SEM 图和 XRD 图; (d) 铜微电极方阻随激光功率变化曲线, 插图: 铜微电极所制备 LED 电路照片^[39]

Fig. 3 (a) Manufacturing process of femtosecond laser reduction based on Cu ionic precursor; (b), (c) SEM images and XRD pattern of Cu microelectrode prepared with different laser powers; (d) Copper microelectrode sheet resistance change curve with laser power, inset: photograph of the LED circuit prepared from Cu microelectrode^[39]

极限低至 10^{-9} M。相较于纯 Ag, Ag/Pd 合金纳米结构具有更好的抗氧化性能, 在 20 天的有氧条件下, 增强因子仍能保持在 1.89×10^8 的较高水平, 具有长期使用的潜力。

2.2.2 还原氧化石墨烯

还原氧化石墨烯由于其低密度、高比表面积, 独特的电学、力学及光学性能, 受到了柔性器件领域研究人员的广泛关注^[81-82]。飞秒激光可实现氧化石墨烯(GO)的还原得到还原氧化石墨烯(rGO)^[83], 过程涉及光化学反应、光热反应和光烧蚀作用^[84]。Le 等^[85]利用飞秒激光处理涂敷氧化石墨烯(GO)薄膜的PDMS, 实现了 GO 的光还原及 PDMS 的光热分解, 得到具有荷叶状层级结构的导电 rGO/PDMS 复合膜。将复合膜弯曲诱导生成多尺度锯齿状和蜘蛛裂隙状微裂纹结构(图 4(a))。基于荷叶状层级结构及多尺度微裂纹的协同作用, 所制备的 rGO/PDMS 传感器具有超疏水

特性, 高应变灵敏度(8699)、超快响应时间(107 μs)、良好耐久性(>10000 循环), 可实现对可听频率范围(20 Hz~20000 Hz)的声学振动进行检测。将其安装在颈部, 可感知超过可听频率范围的声音信号; 即使在嘈杂环境中, 也可根据声带振动识别不同的语音模式。在不同湿度条件下, GO 表面含氧基团和水分子之间的相互作用会导致 GO 电导率和电容变化, 从而实现 GO 的湿度传感(图 4(b))。在低湿度条件下, 质子电导占主导作用, 传感器阻抗较大; 在高湿度条件下, 离子电导占主导作用, 传感器阻抗降低。An 等^[86]以 GO 为传感材料, 飞秒激光还原氧化石墨烯(rGO)为电极, 一步制备了具有高灵敏度、快速响应及高机械稳定性、基于 4×4 传感器阵列的非接触式电子皮肤(图 4(c))。

飞秒激光还可诱导生成还原氧化石墨烯复合材料, 有效提高超级电容器的性能^[2]。Yuan 等^[87]利用空间

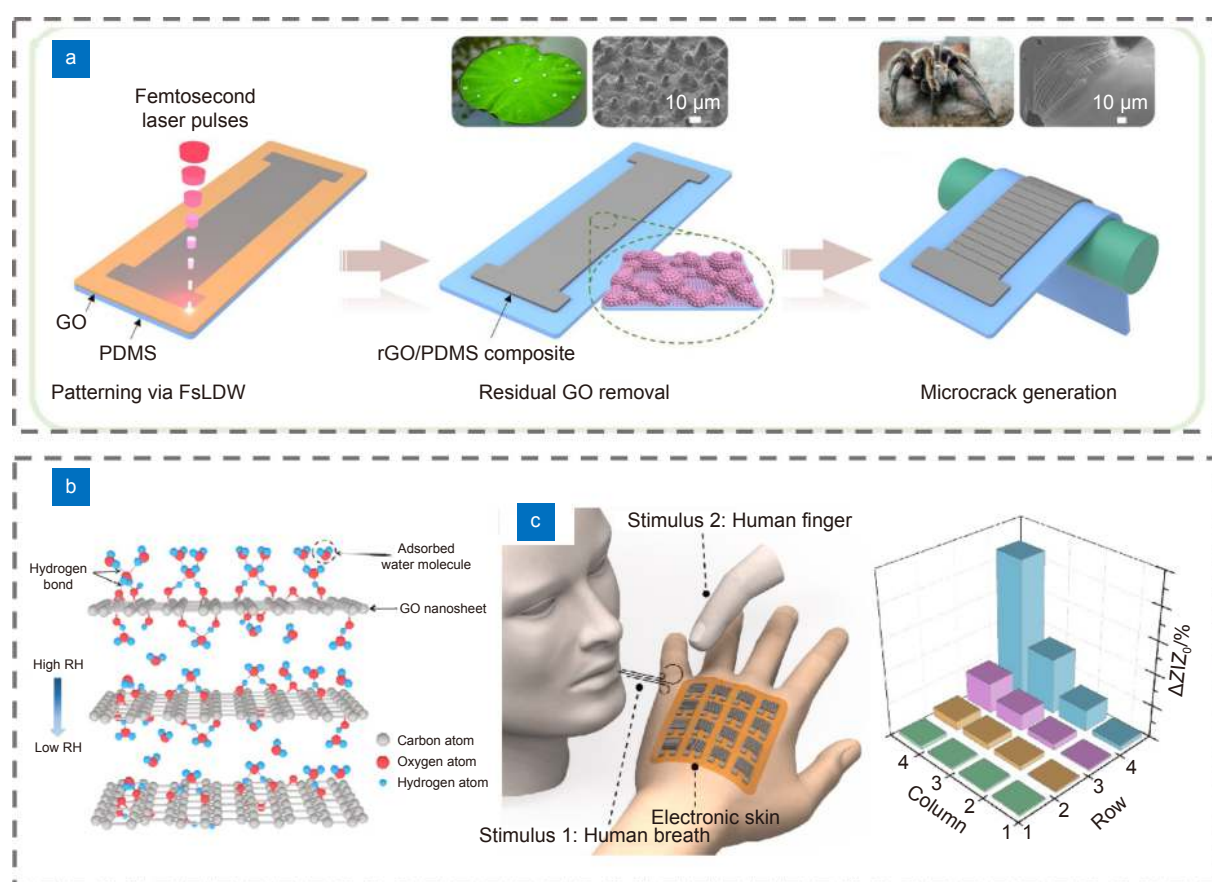


图 4 (a) 飞秒激光制备还原氧化石墨烯/PDMS 复合材料声学传感器制造工艺流程^[85]; (b) 水分子与 GO 纳米片之间相互作用示意图^[86]; (c) 模拟人类皮肤的非接触式湿度传感的电子皮肤原型演示^[86]

Fig. 4 (a) Manufacturing process of femtosecond laser writing rGO/PDMS composite acoustic sensor^[85]; (b) Schematic illustration of the interaction between water molecules and GO nanosheets^[86]; (c) Prototype demonstration of e-skin used for simulation of noncontact sensing properties of human skin^[86]

光调制器 (SLM) 将飞秒激光高斯光束光场调制为平行线、同心圆及叉指的光场 (如图 5(a) 所示), 实现了多种形状还原氧化石墨烯/二氧化锰 (LIG/MnO₂) 柔性微型超级电容器的超快制备。LIG/MnO₂ 的激光还原机理包括光化学及光热还原/氧化 (图 5(b))。在飞秒激光辐照混合物的初始阶段, 光化学还原/氧化占主导作用。飞秒激光在极高峰值功率下可提供大量激发光子形成自由电子及空穴, 促使 GO 还原为 rGO。吸附于 GO 上的 Mn²⁺可促进 GO 的还原, 在此过程中, Mn²⁺吸热氧化形成 MnO₂ 纳米颗粒。随着反应的持续进行, 光热还原/氧化逐渐占主导, GO 热解其含氧官能团分解形成 CO、CO₂ 及 H₂O 并被去除, 使得 GO 还原为 rGO, 同时 Mn²⁺氧化形成 MnO₂。叉指 LIG/MnO₂ 柔性超级电容器较平行线及同心圆的电容器, 电极材

料与电解液接触面积更大、离子扩散路径更短, 电化学性能更优 (图 5(c)), 其面积比电容为 128 mF·cm⁻², 体积比电容为 426.7 F·cm⁻³ (图 5(d))。Li 等^[88] 利用飞秒激光还原 (氧化石墨烯/四氯金酸)GO/HAuCl₄ 混合物得到 rGO/Au 复合材料叉指微电极, 电导率为 1.1×10^6 S·m⁻¹, 相较于 rGO 微电极高 2 个数量级, 说明 Au NPs 的加入可有效提高电极电导率。rGO 的还原电位低于水配位的 AuCl₄⁻, 使得混合物中少量 Au³⁺ 可被带负电荷的 rGO 所提供的电子还原形成 Au 纳米颗粒。相对于连续激光, 飞秒激光可促进微电极中的 HAuCl₄ 和 GO 还原, 且电极中 Au NPs 的连接程度更高, 有效提高了 rGO/Au 微电极的电导率。这使飞秒激光制备的 rGO/Au 微型超级电容器 (0.46 mF·cm⁻²) 较连续激光制备的 rGO/Au 微型超级电容器 (0.20

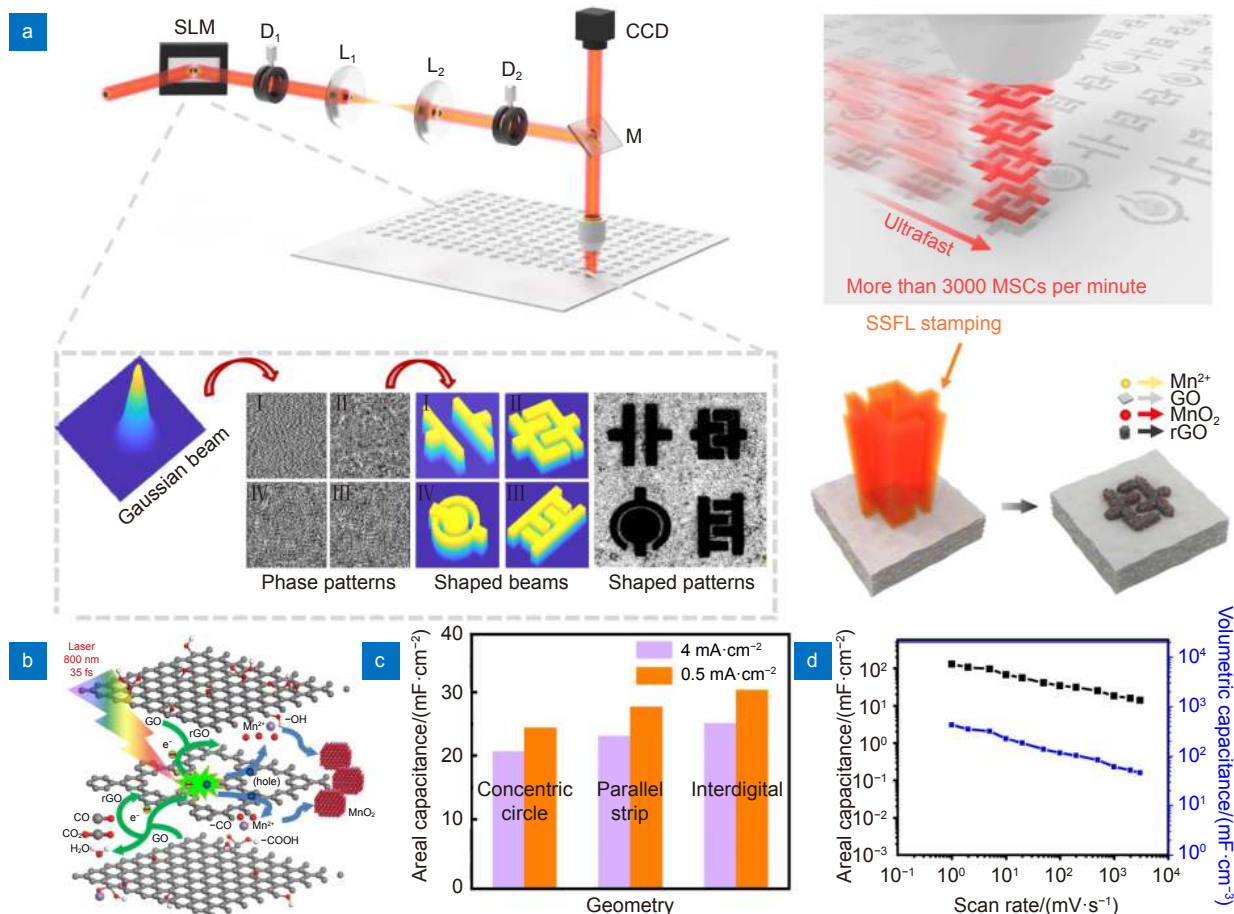


图 5 (a) 利用空间形状的飞秒激光制备 LIG/MnO₂ 超级电容器的示意图; (b) 飞秒激光诱导形成 LIG/MnO₂ 复合材料机理图; (c) 不同形状超级电容器在不同电流密度下的面积比电容; (d) 叉指超级电容器在不同测试扫描速率下的面积比电容及体积比电容^[87]

Fig. 5 (a) Schematics of spatially shaped femtosecond laser strategy to fabricate the graphene/MnO₂ micro-supercapacitors; (b) Schematic diagram of the formation of LIG/MnO₂ composites induced by femtosecond laser; (c) The area-specific capacitance of different geometries under different current density; (d) The areal capacitance and volumetric capacitance of interdigital micro-supercapacitors under different scan rates^[87]

$\text{mF}\cdot\text{cm}^{-2}$)具有更高面积比电容。

2.2.3 高分子材料石墨化及碳化

飞秒激光由于极高的功率密度和瞬时高温高压环境, 可直接将木头、聚酰亚胺(PI)等高分子材料直接石墨化或多孔碳化, 用于柔性电子器件。木头中含有脂肪族和芳香族化合物, 在飞秒激光作用下氧原子形成气态产物, 而剩余的碳原子重新排列形成石墨烯共轭芳香网络^[89]。转化后的石墨烯可转移至柔性PDMS基板上用作高灵敏性柔性石墨烯热敏电阻, 如图6(a)所示^[89], 其热敏电阻是传统铂热敏电阻的16倍, 可应用于电动机金属外壳、曲面玻璃表面及人体部位的实时温度监测。

飞秒激光聚焦部位可诱导多光子吸收使PI局部温度可达1000 K以上, 导致其熔化沸腾、分解及碳化生成多孔碳结构^[92]。In等^[90]利用该工艺制备了柔性良好的全固态微型超级电容器, 如图6(b)所示。研究者系统研究了激光功率、扫描速度及扫描次数对多孔碳结构电导率的影响, 在测试速率为10 mV/s时, 比电容约为800 $\mu\text{F}/\text{cm}^2$ 。Wang等^[92]通过调控飞秒激光物镜与PI基板的距离, 诱导生成多层堆叠的多孔碳结构, 实现了三维微型超级电容器的制造, 在电流密度为0.1 mA/cm^2 时, 面积比电容为42.6 mF/cm^2 。该工作表明: 1)相较于连续激光, 飞秒激光辐照PI可诱导氮/氧原子掺杂的碳结构生成, 有效提高超级电容器的赝电容; 2)相较于单层多孔碳结构, 多层多孔碳结构可提高电极与电解质的接触面积, 有助于提高器件的面积比电容。飞秒激光辐照PI制备的高比表面积多孔碳基结构还可用于传感器^[93], 多孔纳米结构可提高对双酚A(BPA)吸附量, 增加检测灵敏度, 对BPA的检测极限达58.28 aM, 响应时间仅为20 s。还可利用飞秒激光碳化PI构建多功能碳基柔性传感器^[91]: 利用飞秒激光制造了PDMS微结构模版, 将液态PDMS涂于PDMS模版上, 固化、剥离得到具有微结构的PDMS, 并在PDMS上涂敷碳纳米管(CNTs)与飞秒激光碳化PI基板制备的叉指电极组装形成压力传感器。不同压力会改变两个电极间接触面积, 引起传感器电阻变化, 实现负载压力的检测。飞秒激光在PI上制造的多孔碳结构具有类半导体负温度特性, 可用作温度传感器。将其与压力传感器集成便可同时检测外界热刺激和机械刺激, 如图6(c)所示。将两个装有不同质量、不同温度水的小瓶放置于传感器阵列上(图6(d))。根据相对电阻变化, 可同时表征

两个小瓶的温度及压力(图6(e), 6(f))。

2.3 激光诱导纳米连接

合成金属纳米材料后, 通过实现金属纳米材料间的微尺度连接, 可优化所制备微结构的电导率及机械性能, 并改善微结构与柔性基板的附着力, 有助于实现高导电性结构在柔性基板上的制备^[94-95]。直接加热烧结可对金属纳米材料互连, 然而该技术难以实现烧结区域选择性精确调控, 且高温环境极易对柔性热敏基板造成损伤, 限制了其在柔性器件制造中的应用^[96]。

飞秒激光辐照金属纳米材料时, 在纳米材料间隙处产生等离子激元, 使该区域局域加热熔化实现互连^[94], 选择性纳米材料互连可有效避免热敏基板损伤^[97]。Liao等^[39]以Cu纳米颗粒为例, 模拟了飞秒激光辐照下Cu纳米颗粒二聚体周围的电场(图7(a))及温度场(图7(b)), 证明了当电荷极化方向与入射激光偏振方向平行时, 飞秒激光可诱导等离子激元效应, 使Cu纳米颗粒表面极化电荷在颗粒间隙两侧达到最大程度聚集, 此处电场强度得到最大增强($|E/E_0|=34.7$, E 、 E_0 分别为电场强度及入射电场强度)。间隙处强场的形成会增强材料对入射光子的吸收, 成为“热点”, 导致颗粒局域加热, 提高入射激光功率, 可使颗粒“热点”区域的晶格温度升高(图7(c))。由于金属纳米材料的表面效应及尺寸效应, 在远低于块体金属熔点的温度下即可表面熔化实现颗粒连接。基于等离子激元效应的单一纳米线连接可用于高性能传感器开发。Yu等^[99]利用飞秒激光连接铜纳米线(Cu NW)与Ag电极, 实现了柔性单Cu NW葡萄糖传感器的制备。Cu NW与Ag电极的低损伤互连, 在降低其接触电阻的同时没有造成Cu NW的氧化及整体形貌的改变, 使连接后的纳米线仍保持了较高活性, 保证了单Cu NW葡萄糖传感器较高的灵敏度。

等离子激元效应还可用以实现飞秒激光低损伤金属纳米材料互连的柔性透明电极制备。Ha等^[98]利用飞秒激光连接银纳米线(Ag NWs)制备了具有高导电性及高透射率的柔性透明电极。当入射激光能量密度为90 mJ/cm^2 , 扫描速度为0.1 mm/s时, 所制备Ag NWs电极方阻为 $25 \Omega\cdot\text{sq}^{-1}$, 在550 nm下透射率达94%, 较未互连的Ag NWs电极有明显提高(方阻为 $87 \Omega\cdot\text{sq}^{-1}$, 633 nm下透射率为91.3%)(图7(d)、7(e))。图7(f)为飞秒激光连接的银纳米线(Ag NWs)接头的高分辨透射电镜图及选区电子衍射图(SAED), 表明了飞秒激光辐照后只在接头处发生表面熔化连接, 且

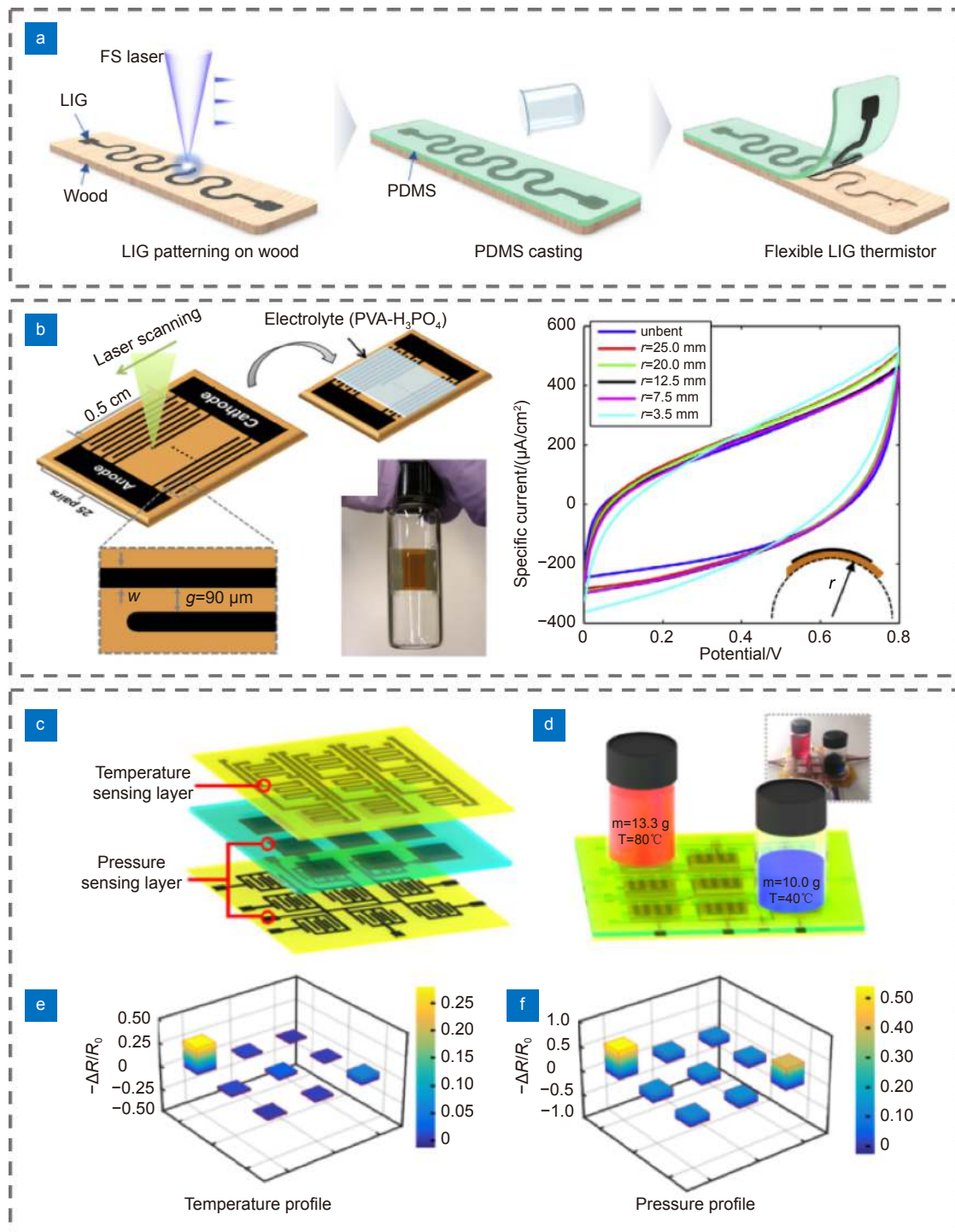


图 6 (a) 飞秒激光直写石墨烯柔性热敏电阻制备方法^[89]; (b) 飞秒激光碳化制备微型超级电容器流程图及照片, 不同弯曲程度的微超级电容器的循环伏安(CV)曲线(扫描速度为1 V/s)^[90]; (c) 飞秒激光微加工法制备传感器阵列原理图^[91]; (d) 传感器阵列同时检测不同物体的温度及压力^[91]; (e) 受温度变化影响的温度传感器的电信号输出^[91]; (f) 受负载压力变化影响的压力传感器的电信号输出^[91]

Fig. 6 (a) Schematic diagram of femtosecond laser direct writing graphene flexible thermistor^[89]; (b) Schematic diagram of fabrication of micro-supercapacitors by femtosecond laser carbonization and photographic image of micro-supercapacitor, cyclic voltammetry (CV) curves of micro-supercapacitors with different bending degrees (the scanning speed is 1 V/s)^[90]; (c) Schematic diagram of sensor array fabricated by femtosecond laser micromachining method^[91]; (d) Sensor array simultaneously detects the temperature and pressure of different objects^[91]; (e) Electrical signal output of the temperature sensor affected by temperature changes^[91]; (f) Electrical signal output of the pressure sensor affected by load pressure changes^[91]

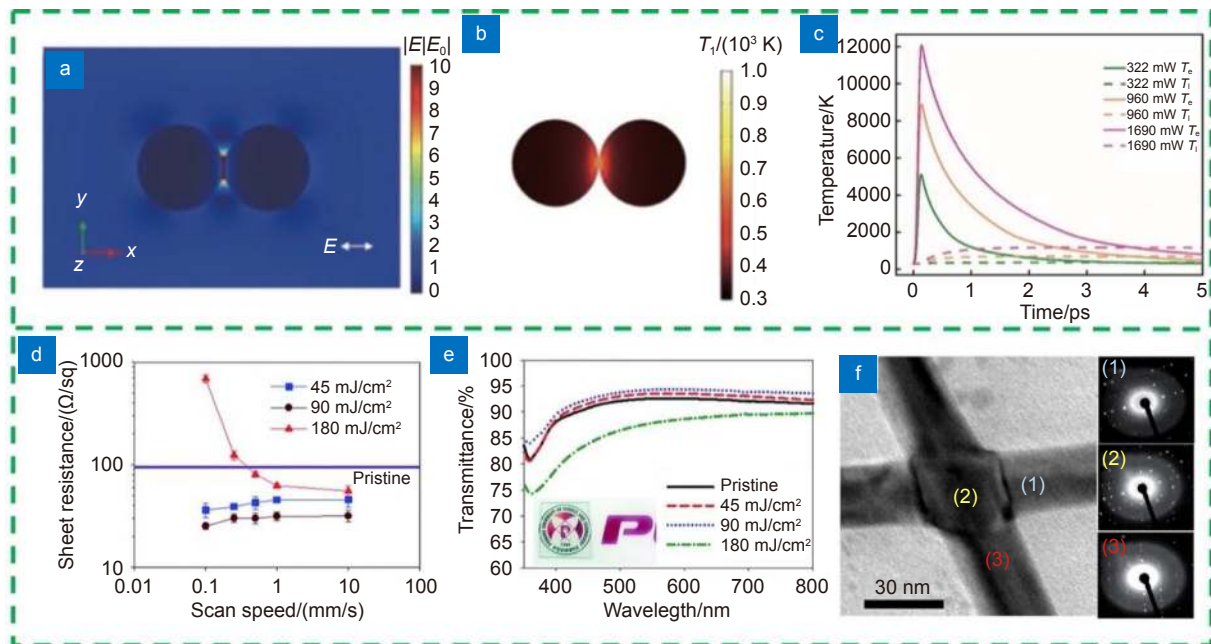


图 7 (a) 960 mW 飞秒激光辐照下 Cu 纳米颗粒二聚体的相对电场增强 ($|E/E_0|$) 分布^[39]; (b) 960 mW 飞秒激光辐照下 Cu 纳米颗粒二聚体在 5 ps 后的温度场分布^[39]; (c) 不同功率单脉冲激光下, 前 5 ps 内 Cu 颗粒电子及晶格温度随时间变化关系^[39]; (d), (e) 飞秒激光辐照前后 Ag NWs 薄膜的方阻变化及透射光谱变化^[98]; (f) 飞秒激光辐照 Ag NW 连接接头及不同部位的 SAED 图案^[98]

Fig. 7 (a) Relative electric field enhancement $|E/E_0|$ distribution of the Cu nanoparticle dimer under 960 mW laser irradiation^[39]; (b) Temperature field distribution of a Cu nanoparticle dimer under 960 mW single pulse laser irradiation after 5 ps^[39]; (c) Relationship between electron and lattice temperature of Cu nanoparticles in the first 5 ps under different laser powers of single pulse laser irradiation^[39]; (d), (e) Sheet resistances and transmittance spectra of Ag NWs films before and after femtosecond laser irradiation^[98]; (f) SAED patterns of Ag NW joints and different parts irradiated by femtosecond laser^[98]

晶格取向和纳米线整体形貌保持不变。该现象同样适用于连接 Ag 纳米颗粒的导电薄膜制备^[24]。由此可见, 飞秒激光纳米连接在低热损伤、低薄膜开裂度的柔性电子器件制备方面潜力巨大。

2.4 飞秒激光电极图案化

飞秒激光电极图案化是利用飞秒激光的烧蚀作用, 将材料多余部分进行高精度选择性去除, 实现电极的灵活图案化制备。Acuautla 等^[100]利用飞秒激光烧蚀工艺选择性图案化去除了沉积于 PI 基板的 Ti/Pt 导电薄膜, 并结合 ZnO 滴涂实现了氨气传感器及微型加热器的集成, 在 300 °C 下对不同氨气浓度 (5 ppm~100 ppm) 均具有较高的检测灵敏度。Schmiedt 等^[101]利用飞秒激光选择性图案化去除了涂敷在 PI 基板的金/铬 (Au/Cr) 薄膜 (厚度 < 50 nm), 获得了柔性应变传感器。研究发现 Au/Cr 薄膜的烧蚀阈值远低于 PI 基板, 可在不损伤 PI 基板的前提下对 Au/Cr 膜进行去除, 展现了飞秒激光在柔性热敏基板超薄金属膜功能图案化方面的优势。

石墨烯电极的图案形状及其分辨率通常影响石墨烯基器件的性能^[102], 飞秒激光烧蚀可实现石墨烯薄膜的高分辨率微观图案化, 满足其在多种柔性器件上的应用^[103]。Ye 等^[104]通过飞秒激光烧蚀将化学气相沉积法 (CVD) 生长的石墨烯薄膜转变为富含多种缺陷的石墨烯基可穿戴多功能传感器。圆形石墨烯阵列由于边界较为平滑, 在拉伸过程中有利于裂纹的生长及扩展, 应变卸载后易恢复至初始状态, 可用于应变传感器 (图 8(a)); 三角形石墨烯阵列由于其三个角边缘更多的悬挂键及空位, 受热时晶格振动剧烈会产生强烈声子-电子散射效应, 所以具有更大的电阻变化, 适用于温度传感器 (图 8(b)); 六边形石墨烯阵列因其较长的周长, 具有更多的边缘悬挂键与 CO 发生反应, 使其具有优异的 CO 气体灵敏度 (图 8(c)), 同时也可用于对湿度的检测 (图 8(d))。将不同石墨烯图形阵列集成于一个透明电子皮肤, 可同时检测人体脉搏、温度及周围有害气体, 方便对人体健康的实时监测。

利用飞秒激光还可实现电极的双面图案化构建,

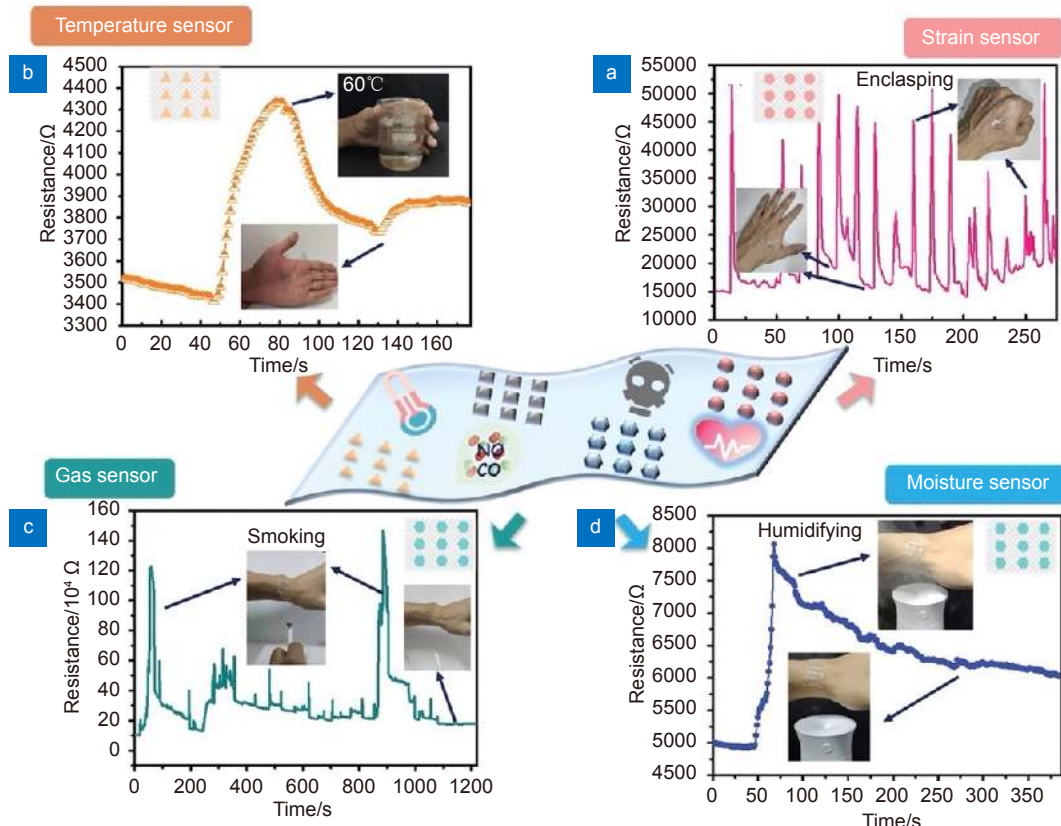


图 8 在 (a) 握紧; (b) 拿乘 ($60\text{ }^\circ\text{C}$) 热水的烧杯; (c) 烟气; (d) 加湿条件下, 不同图案石墨烯传感器的电阻随时间变化^[104]

Fig. 8 Resistance change of graphene sensor with time under the certain conditions: (a) enclasping; (b) holding a beaker with hot water ($60\text{ }^\circ\text{C}$); (c) smoking; (d) humidifying^[104]

有利于高度集成柔性电子器件的开发。Li 等^[105]利用飞秒激光在柔性透明 PET 基板两侧同步刻蚀完成了背对背、高精度对准 MXene 微型超级电容器的双面构建, 如图 9(a) 所示。利用激光在超级电容器电极上钻通孔, 滴入银浆可实现双面超级电容器的串并联, 最后在电极表面涂敷凝胶电解质便可构建 MXene 微型超级电容器。飞秒激光刻蚀的叉指电极间隙窄, 边缘 MXene 材料向 TiO_2 氧化相转化程度小, 所以多数 MXene 的电化学活性得以保留。图 9(b) 为利用该工艺制作的由 12 个螺旋形超级电容器单元组成的“花瓣”图案双面超级电容器。通过控制微型超级电容器单元数量并设计单元之间串联及并联结构, 可在有限的基板面积上实现对超级电容器工作电压 ($0.6\text{ V} \sim 7.2\text{ V}$) 及电容的调控。

2.5 飞秒激光表面织构化

摩擦纳米发电机 (TENG) 是利用接触/摩擦起电和静电感应将机械能转换为电能的微/纳机电动力系统^[106]。提高摩擦层的表面粗糙度及接触面积有助于

在接触过程中产生更多摩擦电荷并提高电容及有效介电常数, 是提高 TENG 性能的有效手段之一^[107], 可通过飞秒激光微纳织构实现。Huang 等^[108]利用飞秒激光在 Cu 薄膜表面烧蚀制备锥状微米结构和纳米颗粒的复合微/纳结构, 并利用单脉冲飞秒激光在 PDMS 表面烧蚀得到了微碗状结构, 以上述两种结构作为摩擦层, 以丙烯酸片作为支撑层组装形成了 TENG, 制备流程如图 10(a) 所示。改变飞秒激光功率可调控 PDMS 上微碗状结构的尺寸, 实现摩擦层接触面积的调控。在 $10\text{ M}\Omega$ 下瞬时输出功率可达 $13.99\text{ }\mu\text{W}$, 是无微纳结构 TENG 器件的 21 倍。这项工作表明具有微纳结构的摩擦层, 摩擦电荷更易分离, 并易在层间形成更大的偶极矩, 提升 TENG 的输出电性能。

Kim 等^[27]制备了包含飞秒激光微纳织构的 PDMS 摩擦层的 TENG 器件, 研究了不同激光功率下微纳结构对 TENG 性能的影响。激光功率为 29 mW 可在 PDMS 表面形成规则的凹半球结构, 而功率超过 50 mW 则会在深凹半球结构上形成不规则亚微米粗糙表面,

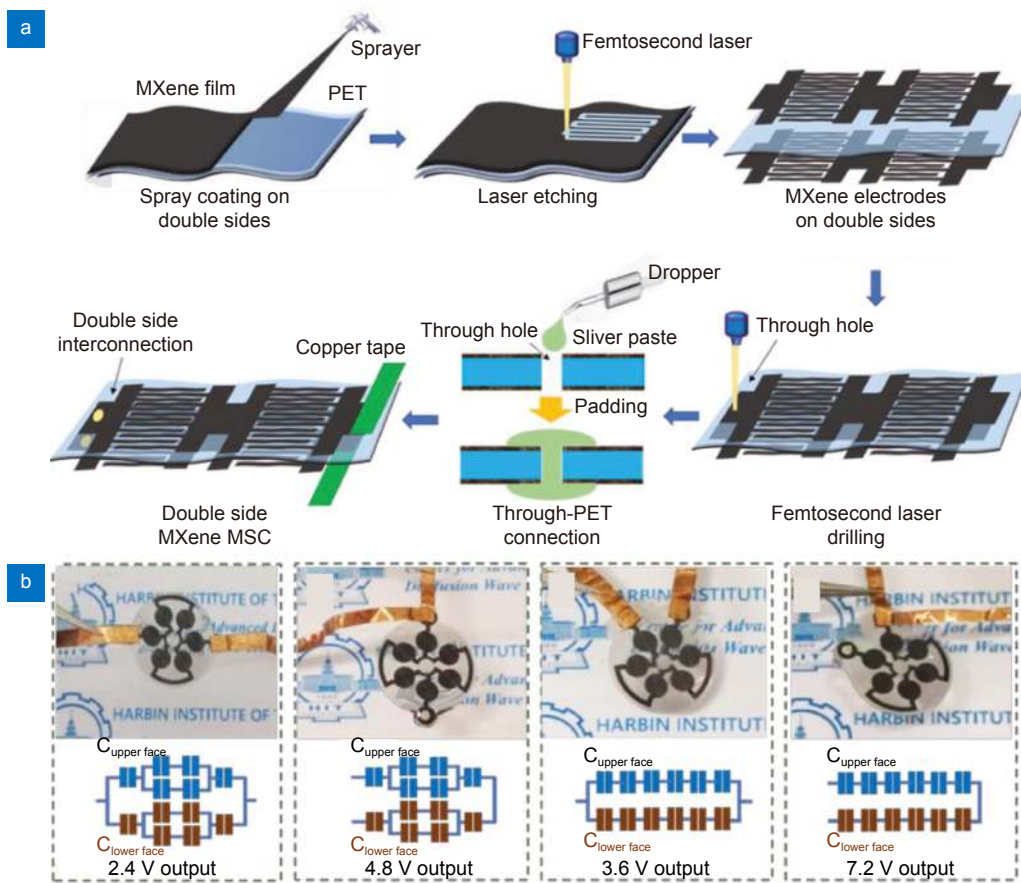


图 9 (a) 飞秒激光一步刻蚀制备双面微型超级电容器工艺流程图;
 (b) 12 螺旋形单元间不同连接方式组成的“花瓣”图案超级电容器的照片^[105]

Fig. 9 (a) Schematic of fabrication of double sided micro-supercapacitors by one-step femtosecond laser etching;
 (b) Photographs of double-side micro-supercapacitors and different connections of twelve spiral units in 'flower petal' pattern^[105]

如图 10(b) 所示。在 29 mW 功率制备下的 TENG 具有最佳性能, 所产生的最大开路电压为 42.5 V, 最大短路电流为 10.1 μ A, 功率密度为 107.3 μ W/cm²。而当功率超过 50 mW 时, 所制备 TENG 的 V_{oc} 及 I_{sc} 随激光功率的增加而急剧下降, 这是由于高功率下制造的 PDMS 表面的不规则凸起使顶部 Al 电极不能与 PDMS 充分接触, TENG 性能变差 (图 10(c)、10(d))。

3 总结与展望

本文综述了飞秒激光液相纳米材料合成、飞秒激光纳米材料还原、飞秒激光诱导纳米连接、飞秒激光电极图案化及飞秒激光表面织构化五种面向柔性电子器件的飞秒激光加工工艺机理及研究现状。激光微纳制造和图案化技术作为一种非接触式技术, 具有加工精度高、可控性强、高效可集成的优势, 在柔性电子器件的制备中极具应用潜力。飞秒激光基于其峰值功率极高、热效应极小等特点, 可有效避免对热敏基板

的热损伤, 有助于实现对可选区的高精细低损加工; 还可实现对材料的成分、结构的大体可控调节, 为多功能、高集成化及高性能的柔性电子器件的开发提供多种可能。飞秒激光液相材料合成可实现多种材料的制备, 可以取代化学合成的材料用于柔性器件的构造, 其卓越的活性更易于获得更高性能的柔性电子器件。

飞秒激光微纳加工工艺已经显现出制备柔性电子器件的广泛应用前景, 但仍存在一些技术挑战:

1) 飞秒激光与材料的相互作用机理尚未完全明确: 飞秒激光液相材料合成的具体过程和机理仍需深入研究, 比如光致液体分子分解和靶材原子化/离子化, 非线性光学效应对激光特性的影响等; 飞秒激光诱导纳米同质材料和异质材料连接及跨尺度互连行为仍需深入理论支撑和实验探索以及应用拓展。

2) 飞秒激光诱导制备的微纳结构受多方因素影响, 利用飞秒激光精确调控电极材料的化学成分和微/纳观结构难度较大, 目前所面临的挑战是产物多为多组

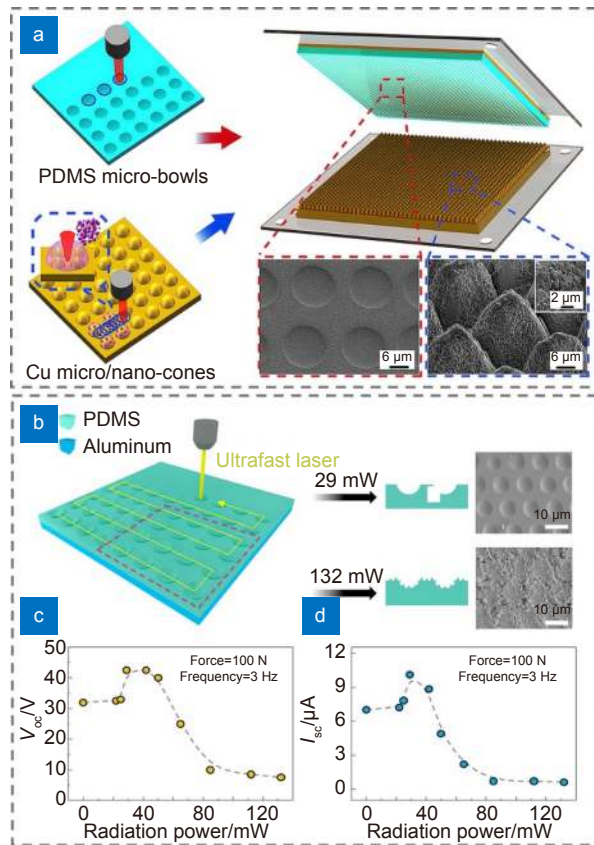


图 10 飞秒激光烧蚀的 Cu 微/纳锥结构及 PDMS 微碗状结构制备的 TENG 的制造工艺流程图^[108]; (b) 飞秒激光辐照制备 PDMS 摩擦层的示意图, 29 mW 和 132 mW 激光功率下制备的 PDMS 的 SEM 图像^[27]; 0 ~ 132 mW 激光功率范围内制备的 TENGs 的 (c) 开路电压及 (d) 短路电流^[27]

Fig. 10 Schematic of the fabrication process of TENG prepared by femtosecond laser ablation of Cu micro/nano-cones and PDMS micro-bowl^[108]; (b) Schematic illustration of the fabrication of the PDMS by femtosecond laser irradiation and SEM images of the PDMS at laser power of 29 mW and 132 mW^[27]; (c) open-circuit voltage (d) short-circuit current of the fabricated TENGs with laser power ranging from 0 to 132 mW^[27]

分复合结构^[75-76], 所得碳结构孔径不均匀^[87,92]和纳米颗粒粒径范围大^[39,77]。

3) 从柔性电子器件制备的角度来说, 相较于分步制造法, 飞秒激光虽然可快速一步制备柔性器件, 但对所得电极材料的成分、结构精确调控更难, 使器件性能的进一步优化提升受到阻碍。多功能集成柔性器件是未来重要发展方向, 飞秒激光制备柔性器件目前面临功能“多而不精”的问题, 亟需优化每种功能器件性能并探索其最优设计和布局^[1]。目前, 利用飞秒激光制备纳米发电机与功能电子设备集成的自供电柔性器件报道仍较少, 这是由于飞秒激光制备的纳米发电机性能仍有待提高, 驱动多功能集成的柔性器件, 并同时进行数据处理、传输及可视化仍是一个挑战^[109-110]。在逐渐提升纳米发电机性能的同时, 将大容量储能设备(超级电容器)与高性能纳米发电机相互

集成可能是解决多功能柔性电子器件一体化自供电的潜在解决方案。

利益冲突: 所有作者声明无利益冲突

参考文献

- Xu K C, Lu Y Y, Takei K. Multifunctional skin-inspired flexible sensor systems for wearable electronics[J]. *Adv Mater Technol*, 2019, 4(3): 1800628.
- Wan Z F, Chen X, Gu M. Laser scribed graphene for supercapacitors[J]. *Opto-Electron Adv*, 2021, 4(7): 200079.
- Park J, Hwang J C, Kim G G, et al. Flexible electronics based on one-dimensional and two-dimensional hybrid nanomaterials[J]. *InfoMat*, 2020, 2(1): 33–56.
- Abid N, Khan A M, Shujait S, et al. Synthesis of nanomaterials using various top-down and bottom-up approaches, influencing factors, advantages, and disadvantages: a review[J]. *Adv Colloid Interface Sci*, 2022, 300: 102597.
- Kim Y U, Kwon N Y, Park S H, et al. Patterned sandwich-type

- silver nanowire-based flexible electrode by photolithography[J]. *ACS Appl Mater Interfaces*, 2021, **13**(51): 61463–61472.
- [6] Choi Y, Seong K D, Piao Y. Metal-organic decomposition ink for printed electronics[J]. *Adv Mater Interfaces*, 2019, **6**(20): 1901002.
- [7] Ahn Y, Lee H, Lee D, et al. Highly conductive and flexible silver nanowire-based microelectrodes on biocompatible hydrogel[J]. *ACS Appl Mater Interfaces*, 2014, **6**(21): 18401–18407.
- [8] Li L H, Gao M, Guo Y Z, et al. Transparent Ag@Au-graphene patterns with conductive stability via inkjet printing[J]. *J Mater Chem C*, 2017, **5**(11): 2800–2806.
- [9] Liao J N, Guo W, Peng P. Direct laser writing of copper-graphene composites for flexible electronics[J]. *Opt Lasers Eng*, 2021, **142**: 106605.
- [10] Zhou W P, Bai S, Ma Y, et al. Laser-direct writing of silver metal electrodes on transparent flexible substrates with high-bonding strength[J]. *ACS Appl Mater Interfaces*, 2016, **8**(37): 24887–24892.
- [11] Wang C P, Chou C P, Wang P C, et al. Flexible graphene-based micro-capacitors using ultrafast laser ablation[J]. *Microelectron Eng*, 2019, **215**: 111000.
- [12] Lin Z Y, Hong M H. Femtosecond laser precision engineering: from micron, submicron, to nanoscale[J]. *Ultrafast Sci*, 2021, **2021**: 9783514.
- [13] Shih C Y, Streubel R, Heberle J, et al. Two mechanisms of nanoparticle generation in picosecond laser ablation in liquids: The origin of the bimodal size distribution[J]. *Nanoscale*, 2018, **10**(15): 6900–6910.
- [14] Zhang D S, Wada H. Laser ablation in liquids for nanomaterial synthesis and applications[M]//Sugioka K. *Handbook of Laser Micro- and Nano-Engineering*. Cham: Springer, 2021: 1–35.
- [15] Zhang D S, Zhang C, Liu J, et al. Carbon-encapsulated metal/metal carbide/metal oxide core-shell nanostructures generated by laser ablation of metals in organic solvents[J]. *ACS Appl Nano Mater*, 2019, **2**(1): 28–39.
- [16] Zhang Y Y, Jiao Y L, Li C Z, et al. Bioinspired micro/nanostructured surfaces prepared by femtosecond laser direct writing for multi-functional applications[J]. *Int J Extrem Manuf*, 2020, **2**(3): 032002.
- [17] Zhang D S, Ranjan B, Tanaka T, et al. Underwater persistent bubble-assisted femtosecond laser ablation for hierarchical micro/nanostructuring[J]. *Int J Extrem Manuf*, 2020, **2**(1): 015001.
- [18] Zhang D S, Wu L C, Ueki M, et al. Femtosecond laser shockwave peening ablation in liquids for hierarchical micro/nanostructuring of brittle silicon and its biological application[J]. *Int J Extrem Manuf*, 2020, **2**(4): 045001.
- [19] Zhang D S, Ranjan B, Tanaka T, et al. Carbonized hybrid micro/nanostructured metasurfaces produced by femtosecond laser ablation in organic solvents for biomimetic antireflective surfaces[J]. *ACS Appl Nano Mater*, 2020, **3**(2): 1855–1871.
- [20] Amendola V, Amans D, Ishikawa Y, et al. Room-temperature laser synthesis in liquid of oxide, metal-oxide core-shells, and doped oxide nanoparticles[J]. *Chem Eur J*, 2020, **26**(42): 9206–9242.
- [21] Arakane S, Mizoshiri M, Hata S. Direct patterning of Cu microstructures using femtosecond laser-induced CuO nanoparticle reduction[J]. *Jpn Appl Phys*, 2015, **54**(6S1): 06FP07.
- [22] Mizoshiri M, Yoshidomi K. Cu patterning using femtosecond laser reductive sintering of CuO nanoparticles under inert gas injection[J]. *Materials*, 2021, **14**(12): 3285.
- [23] Bharati M S S, Soma V R. Flexible SERS substrates for hazardous materials detection: recent advances[J]. *Opto-Electron Adv*, 2021, **4**(11): 210048.
- [24] Noh J, Ha J, Kim D. Femtosecond and nanosecond laser sintering of silver nanoparticles on a flexible substrate[J]. *Appl Surf Sci*, 2020, **511**: 145574.
- [25] Lamberti A, Perrucci F, Caprioli M, et al. New insights on laser-induced graphene electrodes for flexible supercapacitors: tunable morphology and physical properties[J]. *Nanotechnology*, 2017, **28**(17): 174002.
- [26] Zhang D S, Liu R J, Li Z G. Irregular LIPSS produced on metals by single linearly polarized femtosecond laser[J]. *Int J Extrem Manuf*, 2022, **4**(1): 015102.
- [27] Kim D, Tcho I W, Jin I K, et al. Direct-laser-patterned friction layer for the output enhancement of a triboelectric nanogenerator[J]. *Nano Energy*, 2017, **35**: 379–386.
- [28] Zhao L L, Liu Z, Chen D, et al. Laser synthesis and microfabrication of micro/nanostructured materials toward energy conversion and storage[J]. *Nano-Micro Lett*, 2021, **13**(1): 49.
- [29] Bai S, Sugioka K. Recent advances in the fabrication of highly sensitive surface-enhanced raman scattering substrates: nanomolar to attomolar level sensing[J]. *Light Adv Manuf*, 2021, **2**: 13.
- [30] Zhang D S, Sugioka K. Hierarchical microstructures with high spatial frequency laser induced periodic surface structures possessing different orientations created by femtosecond laser ablation of silicon in liquids[J]. *Opto-Electron Adv*, 2019, **2**(3): 190002.
- [31] Zhou R, Lin S D, Ding Y, et al. Enhancement of laser ablation via interacting spatial double-pulse effect[J]. *Opto-Electron Adv*, 2018, **1**(8): 180014.
- [32] Zhang C Y, Zhou W, Geng D, et al. Laser direct writing and characterizations of flexible piezoresistive sensors with microstructures[J]. *Opto-Electron Adv*, 2021, **4**(4): 200061.
- [33] Xie X, Zhou C, Wei X, et al. Laser machining of transparent brittle materials: from machining strategies to applications[J]. *Opto-Electron Adv*, 2019, **2**(1): 180017.
- [34] Peng P, Li L H, He P, et al. One-step selective laser patterning of copper/graphene flexible electrodes[J]. *Nanotechnology*, 2019, **30**(18): 185301.
- [35] Park S, Lee H, Kim Y J, et al. Fully laser-patterned stretchable microsupercapacitors integrated with soft electronic circuit components[J]. *NPG Asia Mater*, 2018, **10**(10): 959–969.
- [36] Zang X N, Shen C W, Chu Y, et al. Laser-induced molybdenum carbide-graphene composites for 3D foldable paper electronics[J]. *Adv Mater*, 2018, **30**(26): 1800062.
- [37] Ba H, Sutter C, Papaefthimiou V, et al. Foldable flexible electronics based on few-layer graphene coated on paper composites[J]. *Carbon*, 2020, **167**: 169–180.
- [38] Theodorakos I, Zacharatos F, Geremia R, et al. Selective laser sintering of Ag nanoparticles ink for applications in flexible electronics[J]. *Appl Surf Sci*, 2015, **336**: 157–162.
- [39] Liao J N, Wang X D, Zhou X W, et al. Joining process of copper nanoparticles with femtosecond laser irradiation[J]. *Chin J Lasers*, 2021, **48**(8): 0802008.

廖嘉宁, 王欣达, 周兴汶, 等. 铜纳米颗粒的飞秒激光连接过程研

- 究[J]. *中国激光*, 2021, **48**(8): 0802008.
- [40] An J N, Le T S D, Lim C H J, et al. Single-step selective laser writing of flexible photodetectors for wearable optoelectronics[J]. *Adv Sc*, 2018, **5**(8): 1800496.
- [41] Sakka T, Saito K, Ogata Y H. Confinement effect of laser ablation plume in liquids probed by self-absorption of C₂ Swan band emission[J]. *J Appl Phys*, 2005, **97**(1): 014902.
- [42] Zhang D S, Gökce B, Barcikowski S. Laser synthesis and processing of colloids: fundamentals and applications[J]. *Chem Rev*, 2017, **117**(5): 3990–4103.
- [43] Zhang D S, Li Z G, Sugioka K. Laser ablation in liquids for nanomaterial synthesis: diversities of targets and liquids[J]. *J Phys Photonics*, 2021, **3**(4): 042002.
- [44] Zhang D S, Liu J, Liang C H. Perspective on how laser-ablated particles grow in liquids[J]. *Sci China Phys Mechan Astron*, 2017, **60**(7): 074201.
- [45] Li S H, Li Y, Liu K, et al. Laser fabricated carbon quantum dots in anti-solvent for highly efficient carbon-based perovskite solar cells[J]. *J Colloid Interface Sci*, 2021, **600**: 691–700.
- [46] Shabalina A V, Svetlichnyi V A, Kulich S A. Green laser ablation-based synthesis of functional nanomaterials for generation, storage, and detection of hydrogen[J]. *Curr Opin Green Sustain Chem*, 2022, **33**: 100566.
- [47] Charipar K, Kim H, Piqué A, et al. ZnO nanoparticle/graphene hybrid photodetectors via laser fragmentation in liquid[J]. *Nanomaterials*, 2020, **10**(9): 1648.
- [48] Jian J, Xu Y X, Yang X K, et al. Embedding laser generated nanocrystals in BiVO₄ photoanode for efficient photoelectrochemical water splitting[J]. *Nat Commun*, 2019, **10**(1): 2609.
- [49] Nikolov A S, Stankova N E, Karashanova D B, et al. Synergistic effect in a two-phase laser procedure for production of silver nanoparticles colloids applicable in ophthalmology[J]. *Opt Laser Technol*, 2021, **138**: 106850.
- [50] Suehara K, Takai R, Ishikawa Y, et al. Reduction mechanism of transition metal oxide particles in thermally induced nanobubbles during pulsed laser melting in ethanol[J]. *Chemphyschem*, 2021, **22**(7): 675–683.
- [51] Zhang D S, Liu J, Li P F, et al. Recent advances in surfactant-free, surface-charged, and defect-rich catalysts developed by laser ablation and processing in liquids[J]. *ChemNanoMat*, 2017, **3**(8): 512–533.
- [52] Menéndez-Manjón A, Wagener P, Barcikowski S. Transfer-matrix method for efficient ablation by pulsed laser ablation and nanoparticle generation in liquids[J]. *J Phys Chem C*, 2011, **115**(12): 5108–5114.
- [53] Zhang S D, Gökce B, Sommer S, et al. Debris-free rear-side picosecond laser ablation of thin germanium wafers in water with ethanol[J]. *Appl Surf Sci*, 2016, **367**: 222–230.
- [54] Tan D Z, Zhou S F, Qiu J R, et al. Preparation of functional nanomaterials with femtosecond laser ablation in solution[J]. *J Photochem Photobiol C Photochem Rev*, 2013, **17**: 50–68.
- [55] Anisimov S I, Kapeliovich B L, Perel'man T L. Electron emission from metal surfaces exposed to ultra-short laser pulses[J]. *Zh Eksp Teor Fiz*, 1974, **66**(776): 776–781.
- [56] Xiao J, Liu P, Wang C X, et al. External field-assisted laser ablation in liquid: An efficient strategy for nanocrystal synthesis and nanostructure assembly[J]. *Prog Mater Sc*, 2017, **87**: 140–220.
- [57] Qi L T, Nishii K, Yasui M, et al. Femtosecond laser ablation of sapphire on different crystallographic facet planes by single and multiple laser pulses irradiation[J]. *Opt Lasers Eng*, 2010, **48**(10): 1000–1007.
- [58] Werner D, Hashimoto S. Improved working model for interpreting the excitation wavelength- and fluence-dependent response in pulsed laser-induced size reduction of aqueous gold nanoparticles[J]. *J Phys Chem C*, 2011, **115**(12): 5063–5072.
- [59] Lorazo P, Lewis L J, Meunier M. Short-pulse laser ablation of solids: from phase explosion to fragmentation[J]. *Phys Rev Lett*, 2003, **91**(22): 225502.
- [60] Shih C Y, Wu C P, Shugaev M V, et al. Atomistic modeling of nanoparticle generation in short pulse laser ablation of thin metal films in water[J]. *J Colloid Interface Sci*, 2017, **489**: 3–17.
- [61] Lasemi N, Rupprechter G, Liedl G, et al. Near-infrared femtosecond laser ablation of Au-coated Ni: effect of organic fluids and water on crater morphology, ablation efficiency and hydrodynamic properties of NiAu nanoparticles[J]. *Materials*, 2021, **14**(19): 5544.
- [62] von der Linde D, Schüler H. Breakdown threshold and plasma formation in femtosecond laser–solid interaction[J]. *J Opt Soc Am B*, 1996, **13**(1): 216–222.
- [63] König J, Nolte S, Tünnermann A. Plasma evolution during metal ablation with ultrashort laser pulses[J]. *Opt Express*, 2005, **13**(26): 10597–10607.
- [64] Yan Z J, Chrisey D B. Pulsed laser ablation in liquid for micro-/nanostructure generation[J]. *J Photochem Photobiol C Photochem Rev*, 2012, **13**(3): 204–223.
- [65] De Giacomo A, Dell'Aglio M, Santagata A, et al. Cavitation dynamics of laser ablation of bulk and wire-shaped metals in water during nanoparticles production[J]. *Phys Chem Chem Phys*, 2013, **15**(9): 3083–3092.
- [66] Zhang D S, Choi W, Jakobi J, et al. Spontaneous shape alteration and size separation of surfactant-free silver particles synthesized by laser ablation in acetone during long-period storage[J]. *Nanomaterials*, 2018, **8**(7): 529.
- [67] Tan D Z, Teng Y, Liu Y, et al. Preparation of zirconia nanoparticles by pulsed laser ablation in liquid[J]. *Chem Lett*, 2009, **38**(11): 1102–1103.
- [68] Amans D, Diouf M, Lam J, et al. Origin of the nano-carbon allotropes in pulsed laser ablation in liquids synthesis[J]. *J Colloid Interface Sci*, 2017, **489**: 114–125.
- [69] Dhanunjaya M, Byram C, Vendamani V S, et al. Hafnium oxide nanoparticles fabricated by femtosecond laser ablation in water[J]. *Appl Phys A*, 2019, **125**(1): 74.
- [70] Camarda P, Vaccaro L, Sciortino A, et al. Synthesis of multi-color luminescent ZnO nanoparticles by ultra-short pulsed laser ablation[J]. *Appl Surf Sci*, 2020, **506**: 144954.
- [71] Liu K W, Sakurai M, Aono M. ZnO-based ultraviolet photodetectors[J]. *Sensors*, 2010, **10**(9): 8604–8634.
- [72] Mitra S, Aravindh A, Das G, et al. High-performance solar-blind flexible deep-UV photodetectors based on quantum dots synthesized by femtosecond-laser ablation[J]. *Nano Energy*, 2018, **48**: 551–559.
- [73] Huang Y J, Xie X Z, Li M N, et al. Copper circuits fabricated on flexible polymer substrates by a high repetition rate femtosecond laser-induced selective local reduction of copper oxide nanoparticles[J]. *Opt Express*, 2021, **29**(3): 4453–4463.
- [74] Lee H, Yang M Y. Effect of solvent and PVP on electrode conductivity in laser-induced reduction process[J]. *Appl Phys A*, 2015, **119**(1): 317–323.
- [75] Mizoshiri M, Hata S. Direct writing of Cu-based micro-

- temperature sensors onto glass and Poly(dimethylsiloxane) substrates using femtosecond laser reductive patterning of CuO nanoparticles[J]. *Res Rev J Mater Sci*, 2016, 4(4): 47–54.
- [76] Mizoshiri M, Ito Y, Arakane S, et al. Direct fabrication of Cu/Cu₂O composite micro-temperature sensor using femtosecond laser reduction patterning[J]. *Jpn Appl Phys*, 2016, 55(6S1): 06GP05.
- [77] Liao J N, Wang X D, Zhou X W, et al. Femtosecond laser direct writing of copper microelectrodes[J]. *Chin J Lasers*, 2019, 46(10): 1002013.
廖嘉宁, 王欣达, 周兴汶, 等. 飞秒激光直写铜微电极研究[J]. *中国激光*, 2019, 46(10): 1002013.
- [78] Ferreira P H D, Vivas M G, De Boni L, et al. Femtosecond laser induced synthesis of Au nanoparticles mediated by chitosan[J]. *Opt Express*, 2012, 20(1): 518–523.
- [79] Barton P, Mukherjee S, Prabha J, et al. Fabrication of silver nanostructures using femtosecond laser-induced photoreduction[J]. *Nanotechnology*, 2017, 28(50): 505302.
- [80] Ma Z C, Zhang Y L, Han B, et al. Femtosecond laser direct writing of plasmonic Ag/Pd Alloy nanostructures enables flexible integration of robust SERS substrates[J]. *Adv Mater Technol*, 2017, 2(6): 1600270.
- [81] Soni M, Kumar P, Pandey J, et al. Scalable and site specific functionalization of reduced graphene oxide for circuit elements and flexible electronics[J]. *Carbon*, 2018, 128: 172–178.
- [82] Guan H, Meng J W, Cheng Z Y, et al. Processing natural wood into a high-performance flexible pressure sensor[J]. *ACS Appl Mater Interfaces*, 2020, 12(41): 46357–46365.
- [83] Wan Z F, Streed E W, Lobino M, et al. Laser-reduced graphene: synthesis, properties, and applications[J]. *Adv Mater Technol*, 2018, 3(4): 1700315.
- [84] Low M J, Lee H, Lim C H J, et al. Laser-induced reduced-graphene-oxide micro-optics patterned by femtosecond laser direct writing[J]. *Appl Surf Sci*, 2020, 526: 146647.
- [85] Dinh Le T S, An J N, Huang Y, et al. Ultrasensitive anti-interference voice recognition by bio-inspired skin-attachable self-cleaning acoustic sensors[J]. *ACS Nano*, 2019, 13(11): 13293–13303.
- [86] An J N, Le T S D, Huang Y, et al. All-graphene-based highly flexible noncontact electronic skin[J]. *ACS Appl Mater Interfaces*, 2017, 9(51): 44593–44601.
- [87] Yuan Y J, Jiang L, Li X, et al. Laser photonic-reduction stamping for graphene-based micro-supercapacitors ultrafast fabrication[J]. *Nat Commun*, 2020, 11(1): 6185.
- [88] Li R Z, Peng R, Kihm K D, et al. High-rate in-plane micro-supercapacitors scribed onto photo paper using *in situ* femtolaser-reduced graphene oxide/Au nanoparticle microelectrodes[J]. *Energy Environ Sci*, 2016, 9(4): 1458–1467.
- [89] Kim Y J, Le T S D, Nam H K, et al. Wood-based flexible graphene thermistor with an ultra-high sensitivity enabled by ultraviolet femtosecond laser pulses[J]. *CIRP Ann*, 2021, 70(1): 443–446.
- [90] Lin J B, Hsia B, Yoo J H, et al. Facile fabrication of flexible all solid-state micro-supercapacitor by direct laser writing of porous carbon in polyimide[J]. *Carbon*, 2015, 83: 144–151.
- [91] Bai J R, Gao Y, Lu C, et al. Femtosecond laser micro-fabricated flexible sensor arrays for simultaneous mechanical and thermal stimuli detection[J]. *Measurement*, 2021, 169: 108348.
- [92] Wang S T, Yu Y C, Li R Z, et al. High-performance stacked in-plane supercapacitors and supercapacitor array fabricated by femtosecond laser 3D direct writing on polyimide sheets[J]. *Electrochim Acta*, 2017, 241: 153–161.
- [93] Cheng C, Wang S T, Wu J, et al. Bisphenol a sensors on polyimide fabricated by laser direct writing for onsite river water monitoring at attomolar concentration[J]. *ACS Appl Mater Interfaces*, 2016, 8(28): 17784–17792.
- [94] Xiao M, Zheng S, Shen D Z, et al. Laser-induced joining of nanoscale materials: processing, properties, and applications[J]. *Nano Today*, 2020, 35: 100959.
- [95] Deng Y B, Bai Y F, Yu Y C, et al. Laser nanojoining of copper nanowires[J]. *J Laser Appl*, 2019, 31(2): 022414.
- [96] Han S, Hong S, Ham J, et al. Fast plasmonic laser nanowelding for a Cu-nanowire percolation network for flexible transparent conductors and stretchable electronics[J]. *Adv Mater*, 2014, 26(33): 5808–5814.
- [97] Lin L C, Xing S L, Huo J P, et al. Research progress of ultrafast laser-induced nanowires joining technology[J]. *Chin J Lasers*, 2021, 48(8): 0802001.
林路婵, 邢松龄, 霍金鹏, 等. 超快激光纳米线连接技术研究进展[J]. *中国激光*, 2021, 48(8): 0802001.
- [98] Ha J, Lee B J, Hwang D J, et al. Femtosecond laser nanowelding of silver nanowires for transparent conductive electrodes[J]. *RSC Adv*, 2016, 6(89): 86232–86239.
- [99] Yu Y C, Deng Y B, Al Hasan M A, et al. Femtosecond laser-induced non-thermal welding for a single Cu nanowire glucose sensor[J]. *Nanoscale Adv*, 2020, 2(3): 1195–1205.
- [100] Acuautla M, Bernardini S, Bendahan M, et al. Ammonia sensing properties of ZnO nanoparticles on flexible substrate[J]. *Int J Smart Sens Intell Syst*, 2020, 7(5): 1–4.
- [101] Schmiedt R E, Qian C, Behr C, et al. Flexible sensors on polyimide fabricated by femtosecond laser for integration in fiber reinforced polymers[J]. *Flex Print Electron*, 2018, 3(2): 025003.
- [102] Das T, Sharma B K, Katiyar A K, et al. Graphene-based flexible and wearable electronics[J]. *J Semicond*, 2018, 39(1): 011007.
- [103] Kalita G, Qi L T, Namba Y, et al. Femtosecond laser induced micropatterning of graphene film[J]. *Mater Lett*, 2011, 65(11): 1569–1572.
- [104] Ye X H, Qi M, Yang Y F, et al. Pattern directive sensing selectivity of graphene for wearable multifunctional sensors via femtosecond laser fabrication[J]. *Adv Mater Technol*, 2020, 5(11): 2000446.
- [105] Li Q, Wang Q Z, Li L L, et al. Femtosecond laser - etched mxene microsupercapacitors with double - side configuration via arbitrary on - and through - substrate connections[J]. *Adv Energy Mater*, 2020, 10(24): 2000470.
- [106] Wang H, Cheng J, Wang Z Z, et al. Triboelectric nanogenerators for human-health care[J]. *Sci Bull*, 2021, 66(5): 490–511.
- [107] Cheng G G, Zhang W, Fang J, et al. Fabrication of triboelectric nanogenerator with textured surface and its electric output performance[J]. *Acta Phys Sin*, 2016, 65(6): 060201.
程广贵, 张伟, 方俊, 等. 基于织构表面的摩擦静电发电机制备及其输出性能研究[J]. *物理学报*, 2016, 65(6): 060201.
- [108] Huang J, Fu X P, Liu G X, et al. Micro/nano-structures-enhanced triboelectric nanogenerators by femtosecond laser direct writing[J]. *Nano Energy*, 2019, 62: 638–644.
- [109] Xiao X Z, Lü C, Wang G, et al. Flexible triboelectric nanogenerator from micro-nano structured polydimethylsiloxane[J]. *Chem Res Chin Univ*, 2015, 31(3): 434–438.

[110] Wang S, Xie G Z, Tai H L, et al. Ultrasensitive flexible self-powered ammonia sensor based on triboelectric

nanogenerator at room temperature[J]. *Nano Energy*, 2018, 51: 231–240.

作者简介



廖嘉宁 (1996-), 女, 上海交通大学材料学院
2021 级博士研究生, 主要从事飞秒激光微纳制
造及其应用相关的研究。
E-mail: zjLiaojianing@163.com



【通信作者】李铸国, 男, 博士, 特聘教授,
上海交通大学上海市激光制造与材料改性重点
实验室主任、材料科学与工程学院副院长。先
后在上海交通大学获学士和硕士学位、日本大
阪大学获工学博士学位。担任国家重点研发计
划项目负责人。主要研究方向为先进激光制造
与控制, 在 *Acta Mater*、*Mater Design*、*Appl
Surf Sci* 等国际著名期刊发表论文 180 余篇,
发表中国科学引文数据库论文 66 篇; 授权国
家发明专利 40 余项。研究成果为我国 核电、
航空航天等领域重大构件的设计与制造做出了
突出贡献, 荣获上海市科技进步奖一等奖、中
国机械工业科学技术奖一等奖、教育部技术发
明奖二等奖等省部级科技奖励 10 项。

E-mail: lizg@sjtu.edu.cn

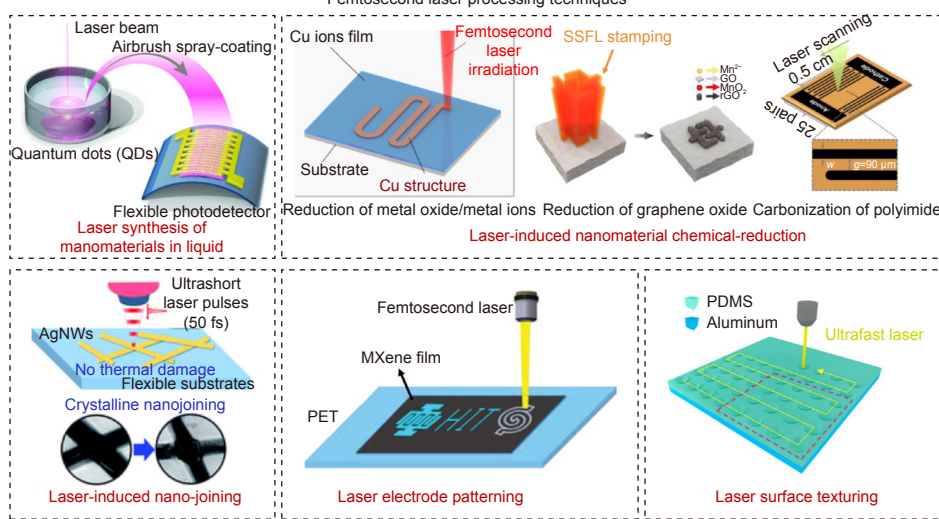


【通信作者】张东石, 男, 博士, 长聘教轨副
教授, 上海交通大学材料学院、焊接与激光制
造研究所飞秒激光微纳加工方向的负责人之一。
本硕博就读于西安交通大学, 随后在德国杜伊
斯堡埃森大学 (University of Duisburg-Essen) 和
日本理化学研究所 (RIKEN) 做博士后研究,
于 2020 年加入上海交通大学李铸国教授团队。
主要研究兴趣包括飞秒激光微纳加工新工艺开
发、新结构制造、新材料合成、新现象探索、
新机理澄清, 目前重点关注多学科交叉融合,
目前发表三十余篇 SCI 文章, H-Index 为 25。
E-mail: zhangdongshi@sjtu.edu.cn

Advance in femtosecond laser fabrication of flexible electronics

Liao Jianing, Zhang Dongshi*, Li Zhuguo*

Femtosecond laser processing techniques



Femtosecond-laser based techniques for the fabrication of flexible electronics

Overview: With the rapid development of information technology and the rise of consumer electronics, flexible electronic devices with high integration, miniaturization and lightweight have attracted wide research attentions. Such flexible electronic devices are typically composed of functional parts, conductive structures, and flexible substrates. The functional parts can respond to external stimuli and convert them into electrical signals. The conductive structures are used for electrical signal transmission and the flexible substrates are used to support functional and conductive structures. The preparation of flexible electronic devices requires nanomaterial synthesis, sintering, processing, and patterning, which is an intrinsically interdisciplinary subject that integrates material science, electronics science, and engineering science.

Laser processing, as a maskless process, is able to realize material synthesis and sintering, surface modification, texturing, patterning, and even develop entire flexible devices in one step. Femtosecond laser, benefiting from an ultrashort pulse width can not only achieve “cold” processing with low-damage high-resolution micro-nano structures, but also realize nanomaterial synthesis and nano-joining of multi-dimensional nanomaterials, showing great potentials for the fabrication of flexible electronics. In this paper, five femtosecond-laser based techniques for the fabrication of flexible electronics are reviewed, including laser synthesis of nanomaterials in liquids, laser-induced nanomaterial chemical-reduction, laser-induced nanojoining, laser electrode patterning, and laser surface texturing. The technique of laser synthesis of nanomaterials in liquids can be classified into laser ablation in liquids (LAL), laser fragmentation in liquids (LFL), laser melting in liquids (LML) and laser defect engineering in liquids (LDL). Specifically, LAL can be used to transform solid targets into functional nanomaterials whose physicochemical properties are manipulable via changing target compositions, liquid molecules, and processing parameters. LFL, LML and LDL are downstream techniques enabling to further tune the properties of LAL-synthesized nanomaterials. Laser synthesized nanomaterials show pure and active properties. They are good candidates to be the alternative of chemically synthesized nanomaterials for the fabrication of high-performance flexible electronic devices. Regarding laser-induced nanomaterial chemical-reduction, the mechanisms are mainly photochemical and photothermal reduction, allowing the transition of metal salts or graphene oxide/high polymer materials or their mixtures into metal, reduced graphene oxide/carbon, or metal/carbon composite electrodes. Femtosecond laser nano-joining, on the basis of laser-induced localized surface plasmonic effect can enhance the local temperature at the contact area between metallic nanoparticles, and facilitate the interconnection of nanoparticles for the fabrication of low-damage flexible conductive electrodes and nanowire sensors. Femtosecond laser ablation can also realize electrode patterning and surface texturing, which have been used for fabrication of flexible electronics including sensors, supercapacitors and triboelectric nanogenerators. In light of high flexibility and strong capacities of femtosecond laser ablation and processing, its extensive applications in flexible electronics can be envisaged to prosper in the near future. However, there are still some challenges ahead, so our perspectives are provided at the end of this review.

Liao J N, Zhang D S, Li Z G. Advance in femtosecond laser fabrication of flexible electronics[J]. Opto-Electron Eng, 2022, 49(2): 210388; DOI: [10.12086/oee.2022.210388](https://doi.org/10.12086/oee.2022.210388)

Foundation item: Research Start-up Fund for Long-term Associate Professor of Shanghai Jiao Tong University (WF220405017)

Shanghai Key Laboratory of Materials Laser Processing and Modification, School of Materials Science and Engineering, Shanghai Jiao Tong University, Shanghai 200240, China

* E-mail: zhangdongshi@sjtu.edu.cn; lizg@sjtu.edu.cn